



Journal homepage: <http://civiljournal.semnan.ac.ir/>

## Shearography-Wavelet-Based Damage Detection Methodology for Aluminum Beams

Amirhossein Abbasi<sup>1</sup>; Mohsen Khatibinia<sup>2</sup>; Hashem Jahangir<sup>3,\*</sup>; José Viriato Araújo Dos Santos<sup>4</sup>; Hernani Miguel Reis Lopes<sup>5</sup>

1. M.Sc. Student, Civil Engineering Department, University of Birjand, Birjand, Iran

2. Associate Professor, Department of Civil Engineering, University of Birjand, Birjand, Iran

3. Assistant Professor, Department of Civil Engineering, University of Birjand, Birjand, Iran

4. Professor of Mechanical Engineering, University of Lisbon, Instituto Superior Tecnico, Lisbon, Portugal

5. Assistant Professor, Department of Mechanical Engineering, DEM-ISEP, Instituto Politécnico do Porto, Porto, Portugal

\* Corresponding author: [h.jahangir@birjand.ac.ir](mailto:h.jahangir@birjand.ac.ir)

### ARTICLE INFO

#### Article history:

Received: 27 December 2022

Revised: 19 January 2023

Accepted: 14 March 2023

#### Keywords:

Shearography method;

Wavelet transform;

Modal rotation;

Modal curvature;

Aluminum beam.

### ABSTRACT

In this paper, aluminum beams in undamaged status and with single and double damage scenarios as slots with the ratio of the slot depth to the beam thickness of 7% and 28% were constructed at the University of Lisbon, Portugal. Then, with the help of the shearography method, the modal rotations of each beam were calculated for the first to third vibration mode shapes. By deriving the modal rotations, the modal strains were obtained and introduced as the input of 22 different families of 2D wavelet transforms with three different scales 1, 7, and 15. Utilizing the wavelet coefficients as damage indices, the results showed that the sensitivity of modal curvatures is higher than other modal data for identifying the location of damages. In addition, among scales 1, 7, and 15, considering scale 7 for wavelet families provides more suitable results. On the other hand, the sinc and isodog wavelet families showed a better ability to reveal the damage location than other wavelets. Investigating the ratio of the maximum value of the wavelet coefficients in the middle part of the beams to the maximum value of the wavelet coefficients in the boundaries showed that among the two selected wavelets, sinc and isodog, the sinc wavelet is more sensitive than the isodog wavelet in identifying damages with obtained results of 0.81, 7.81 and 27.10 for first, second and third damage scenarios, respectively. And therefore, it can be considered the best wavelet for detecting artificial damage in the tested aluminum beams.

### How to cite this article:

Abbasi, A., Khatibinia, M., Jahangir, H., Dos Santos, J. V. A., & Lopes, H. M. R. (2023). Shearography-Wavelet-Based Damage Detection Methodology for Aluminum Beams. *Journal of Rehabilitation in Civil Engineering*, 11(4), 22-43. <https://doi.org/10.22075/jrce.2023.29435.1780>

## 1. Introduction

The damage status of a structure can be identified by changing its inherent characteristics classified as mass, stiffness, and damping. With the help of the modal analysis method, these characteristics can be converted into natural frequencies, mode shapes, and damping ratios [1]. These characteristics can also be obtained experimentally and by conducting modal tests. To perform modal tests on the structure, based on the required accuracy of the test outputs, a grid of points is considered as degrees of freedom on the structure. Then, by applying shocks with a small intensity on each of the degrees of freedom, the vibration responses of the structure are received with the help of sensors placed on the structure [2,3].

Since the mode shapes of a structure simultaneously provide information about its mass and stiffness, they can be a suitable basis for identifying the damaged state of the structure. The presence of damage in structures causes changes in their characteristics [4–6]. Any geometrical and mechanical changes in the structures lead to changes in the mode shapes; therefore, by examining the mode shapes at different times, it is possible to find out the existence of damage in the structures.

In order to obtain the mode shapes with the help of modal tests, impact hammers are used to apply vibration forces to the structures. In addition, the vibration responses of the structure against these shocks are measured with the help of sensors installed on the structure [7].

Since in the modal test, the process of applying impact must be done for all the degrees of freedom, in practice, the number of degrees of freedom of the structure cannot be considered too much, and as a result, the distance between them increases. Increasing the distance between the degrees of freedom of the structure leads to a decrease in the accuracy of the mode shapes received from them. On the other hand, installing the sensor on the structure adds extra weight to the structure, which changes the weight of the structure [8]. In most cases, the effect of sensor weight is ignored in modal tests, which adds to the measurement error of modal data. In addition, in many structural health monitoring operations, it is impossible to access the surface of the existing structure to apply vibration shocks and install sensors [9]. All these cases prompted the researchers to look for new solutions to receive the modal data of structures.

The shearography method is the process of obtaining the modal data of structures without the need to access the surface of the structure, install a sensor and apply vibration shocks to it [10]. In this method, vibration forces are applied to the structure with the help of mechanical sound waves. For this purpose, loudspeakers are used that can send sound waves with desired frequencies toward the structure. The vibration responses of the structure are also measured with the help of microphones placed near the structure and receive the sound waves reflected from the structure's surface [11]. In this method, instead of gridding the structure into degrees of freedom with a predetermined distance, a pattern of points is irradiated on the surface of the structure and with the help of cameras that in short time intervals, they take pictures

of the pattern of points, and their location is recorded. To measure the displacement of all these points due to the collision of sound waves, laser beams were used [12]. The laser projection device shines light rays on the surface of the structure, and by receiving it in the laser sensor, the displacement of each point in the optical pattern is measured.

In the shearography method, the waves sent to the surface of the structure and received from it have a phase difference of  $\Delta\phi$ . This phase difference can be related to the number of displacements created on the surface of the structure  $w(x,y)$  in the horizontal  $x$  and vertical  $y$  direction due to mechanical sound waves. Eq. (1) shows the relationship between the phase difference and the surface displacements of the structure [13]:

$$\Delta\phi(x,y) \approx \frac{4\pi\delta x}{\lambda} \cdot \frac{\partial w(x,y)}{\partial x} \quad (1)$$

In Eq. (1),  $\lambda$  indicates the wavelength of the laser, and  $\delta x$  indicates the size of the selected slices on the image taken from the surface of the structure in the  $x$  direction [16]. Therefore, by considering the mode shapes of a structure as its surface displacements, a relationship between the first derivative of the mode shapes (modal rotation) and the phase difference measured in the shearography process can be established [13]. As a result, by measuring the phase difference in the shearography method, it is possible to access the modal data of the structure without the need to contact the surface of the structure [14].

Although there are many types of research in the field of using wavelets to identify damage in structures [15–20], the number of damage detection researches in which the modal data

is obtained from the shearography method is limited. In the research of Katunin et al. [21], the generalized 1D Maar wavelet was used to detect damages in a beam. In their research, the modal rotations (the first derivative of the shape of the vibration modes) in beams in two states, undamaged and damaged, were obtained from the shearography test and were considered as the input of the Maar wavelet transformation. The results of their research showed that by considering the difference of modal rotations in the damaged and undamaged state as the input of the Maar wavelet, the location of damages can be revealed with more appropriate accuracy [21]. In another study, Katunin et al. [22] identified damages with vertical and oblique slots on beams. They used modal rotations as the input of 1D discrete wavelets by changing the angle of the wavelets in the direction of 45 and 90 degrees. The results showed that the proposed method in their research could not identify fake damage with oblique slots. In another study, dos Santos et al. [23] evaluated damages, including slots with different geometric shapes in a metal plate created as a finite element model (FEM) in ABAQUS software [24]. They obtained the modal rotations of the structure in different states of damage and introduced them as input to transform the generalized 2D wavelet from the 1D B-Spline wavelet. The results showed that using of generalized 1D wavelet can identify damages with different geometric shapes in the numerical model of the metal plate.

## 2. Research significance

Examining the few previous researches in the field of using modal data obtained from shearography tests to identify damage in

structures show that there are many shortcomings and there is a need of improvements in this field. Some of the shortcomings in the background of researches can be categorized as follows:

- In most of the previous research, the used wavelets were 1D wavelets that were applied in horizontal, vertical, or oblique directions on the structures. This shortcoming makes the proposed method unable to detect damages with complicated geometrical shapes. In this case, utilizing 2D wavelets can be helpful.
- In most previous research, a special wavelet family has been used for damage detection. Since there are different families of wavelets with different geometric shapes, it is possible to carry out a comprehensive study on all wavelet families and select the most suitable wavelet family as the optimal damage index can be introduced.

In this research, the experimental modal data were obtained with the help of shearography process to identify the damage in aluminum beams. For this purpose, undamaged and damaged beams are tested by creating slots as damage scenarios in different places of the beams, and their modal rotations were obtained. These modal data were introduced as input to damage indices based on wavelet transform, and the location and severity of artificial damages in beams were estimated. The accuracy of the localization of the estimated damages was compared with the actual damages, and the most appropriate damage index was introduced as a suitable method to identify the damage using the shearography method.

Besides the advantages of shearography method, in some cases, the surface of the structural element is not available or the environmental conditions affect the obtained results, which can be introduced as the limitations and weaknesses of this method.

### 3. Experimental program

#### 3.1. Aluminum beams

In this paper, according to Fig. 1 and Table 1, in the University of Lisbon, Portugal, aluminum beams with a length of 400 mm and a width of 40 mm in four states, including undamaged (B0), with single damage in the middle of the beam length (in length  $X = 200$  mm) with the ratio of the depth of the slot to the thickness of the sheet equal to 7% (B1), with double damages in the middle of the beam (in length  $X = 200$  mm) and on the left side (in length  $X = 64.5$  mm) the beam with the ratio of the depth of the slot to the beam thickness equal to 5% (B2), and having double damage in the middle of the beam (in the length of  $X = 200$  mm) and on the left side (in the length of  $X = 64.5$  mm) were made with the ratio of the depth of the slot to the thickness of the sheet equal to 28% (B3) [25]. Then, with the help of the shearography method, the modal data of each aluminum beam were obtained from modal rotations for the first to third mode shapes. By deriving the modal rotations, the modal curvatures were calculated for each of the mode shapes, which will be used as the input of the damage index. Figs. 2 to 5, respectively, show the modal rotations of beams B0, B1, B2, and B3.

**Table 1.** Geometrical properties of damage scenarios.

Slot	Beam	Damage Location X (mm)	Slot's Depth (mm)	Slot's Width (mm)	Slot's depth to beam's thickness ratio (%)
1	B1	200	0.2	10	7
	B2	200	0.2	10	7
	B3	200	0.85	10	28
2	-	-	-	-	-
	B2	64.5	0.2	10	7
	B3	64.5	0.85	10	28

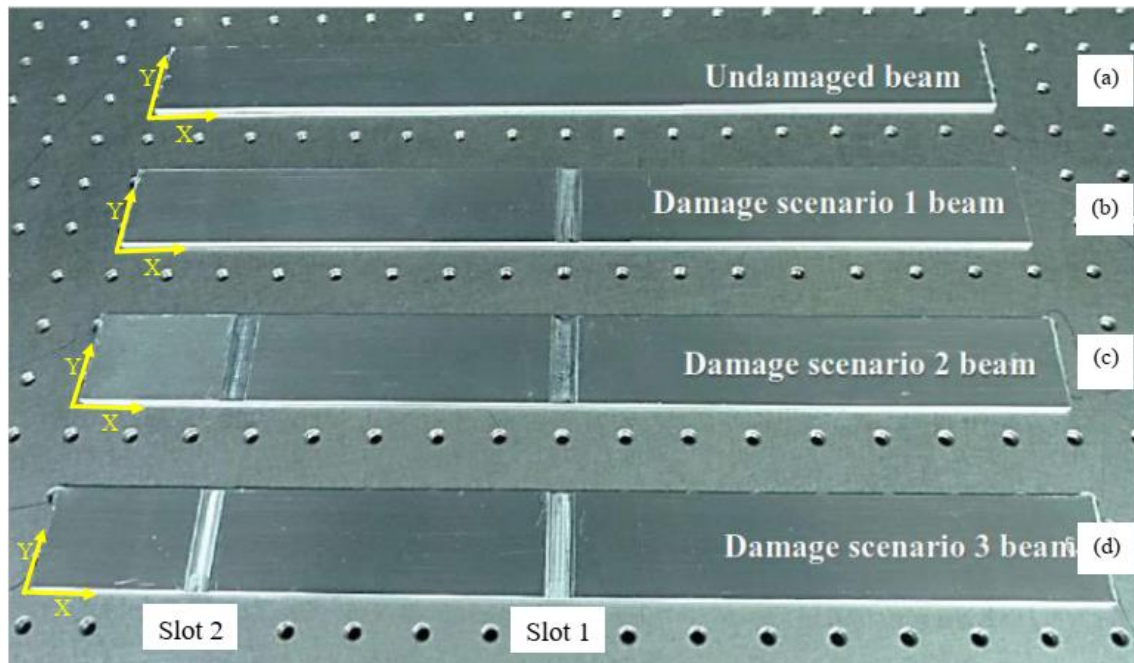


**Fig. 1.** Tested aluminum beams: a) B0; b) B1; c) B2 and d) B3 [25].

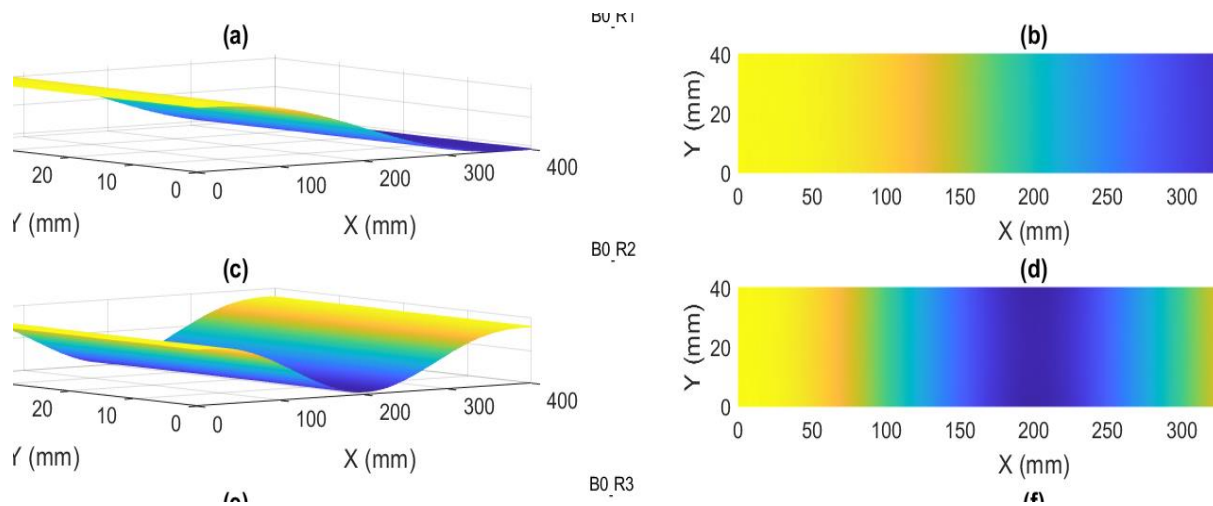


**Fig. 2.** 3D and 2D view of modal rotations in B0: a & b) first model; c & d) second mode and e & f) third mode.

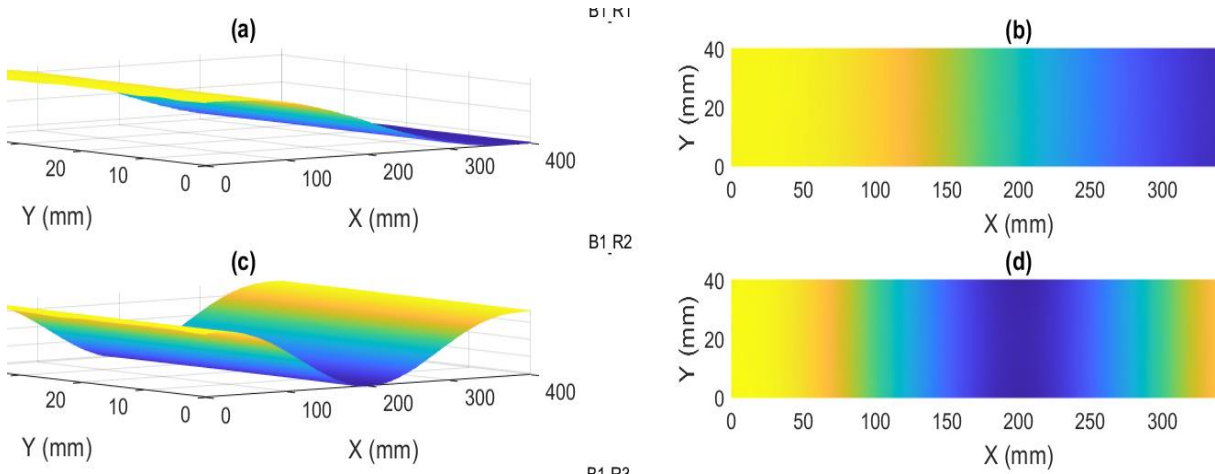


**Fig. 3.** 3D and 2D view of modal rotations in B1: a & b) first model; c & d) second mode and e & f) third mode.

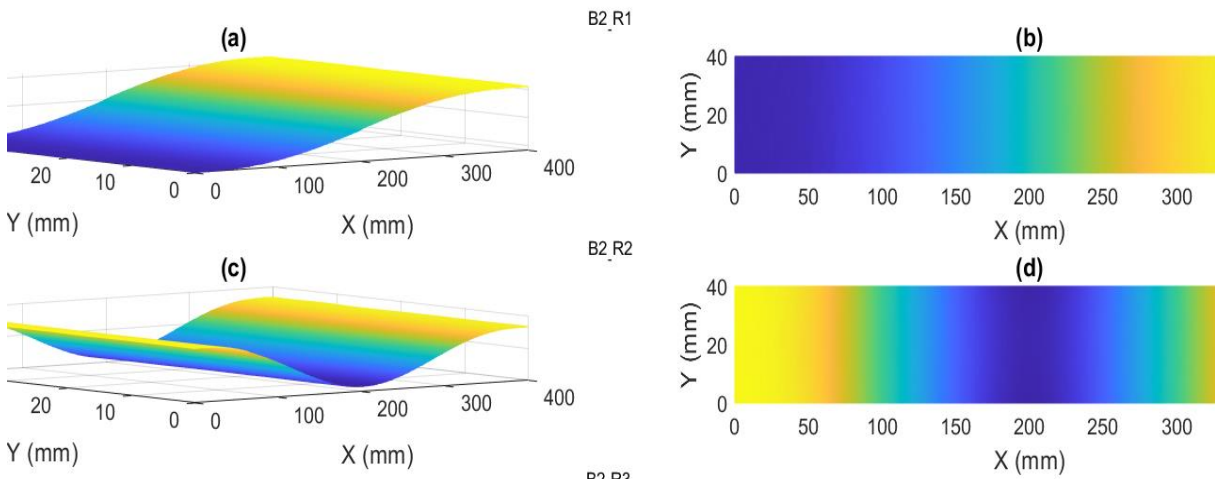


**Fig. 4.** 3D and 2D view of modal rotations in B2: a & b) first model; c & d) second mode and e & f) third mode.

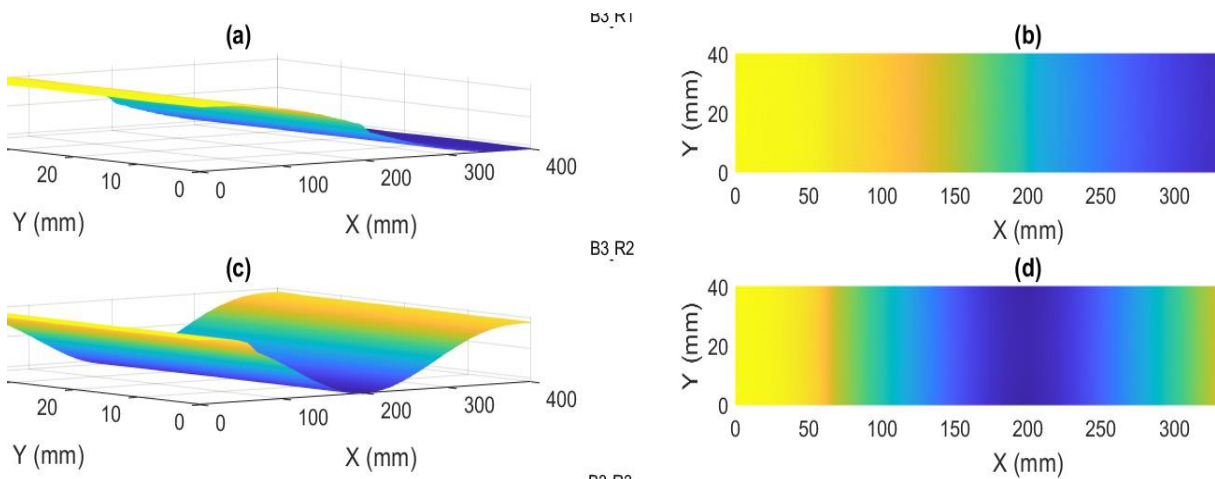


**Fig. 5.** 3D and 2D view of modal rotations in B3: a & b) first model; c & d) second mode and e & f) third mode.



### 3.2. Utilized 2D wavelets

In this research, 2D wavelets including gabmexh, morl, mexh, paul, sinc, dog, cauchy, escauchy, wheel, fan, pethat, dogpow, esmorl, esmexh, gaus, gaus2, gaus3, isodog, dog2, isomorl, rmorl and endstop1 has been used with three different scales of 1, 7 and 15, to identify single and double damage scenarios in beams named B1, B2, and B3. Figs. 6 to 8, respectively, showed the geometric shape of the wavelets used in this paper with scales of 1, 7, and 15.

In this paper, the difference of modal curvatures in beams B1, B2, and B3 with modal curvatures in beam B0, which is considered the base beam, is introduced as the input of each 2D wavelet, and the Wavelet coefficients were used as a damage index to identify the location of damage scenarios in beams B1 to B3. Fig. 9 showcases the overall damage detection process in this paper.

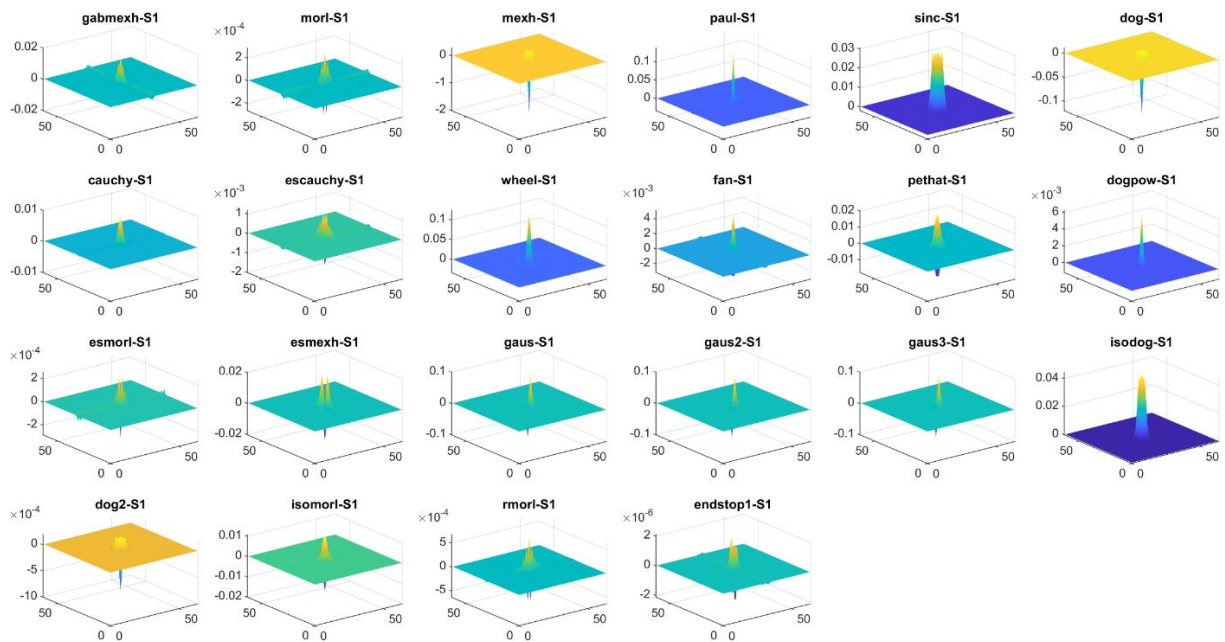


**Fig. 6.** Utilized 2D wavelets with scale 1.

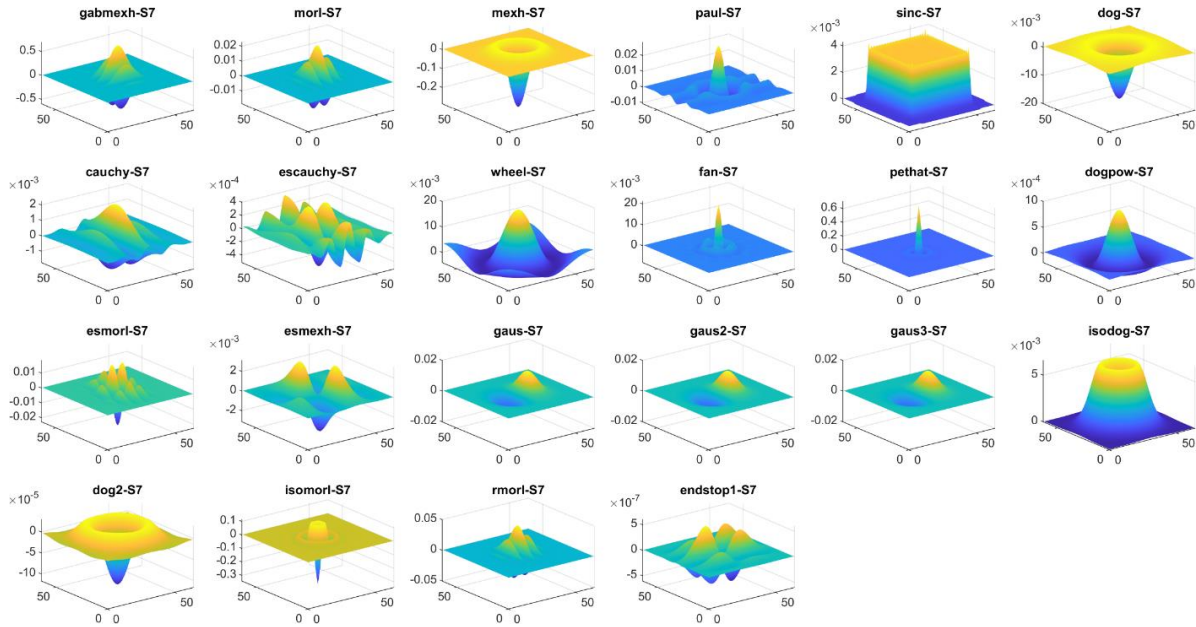


Fig. 7. Utilized 2D wavelets with scale 7.

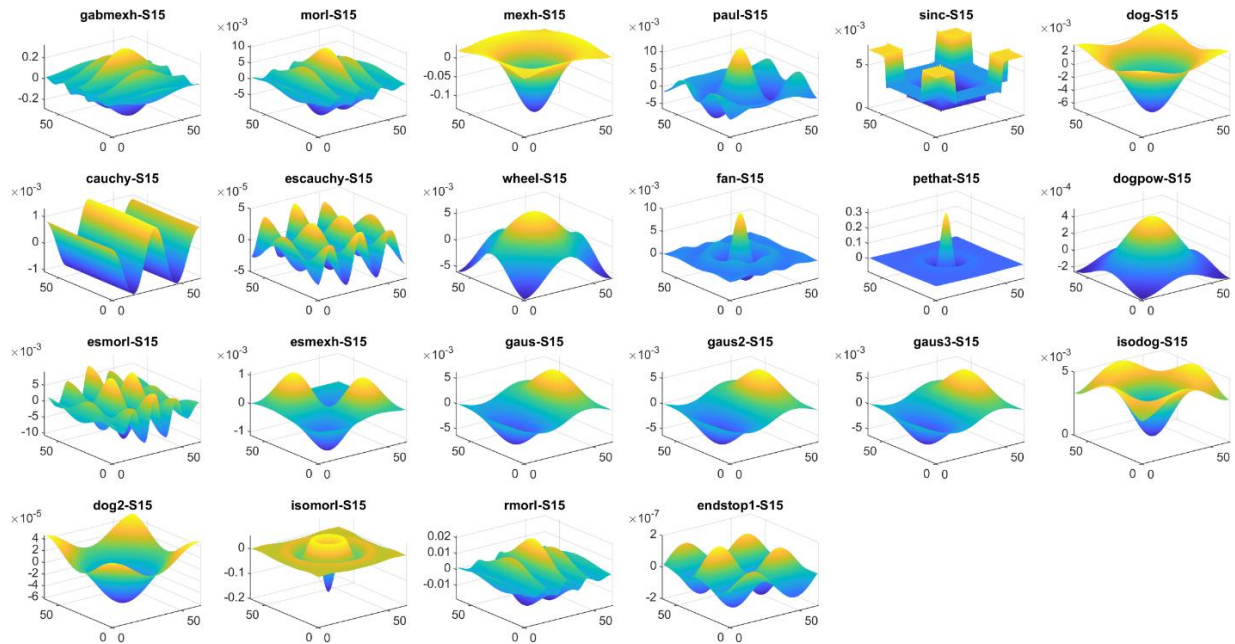


Fig. 8. Utilized 2D wavelets with scale 15.



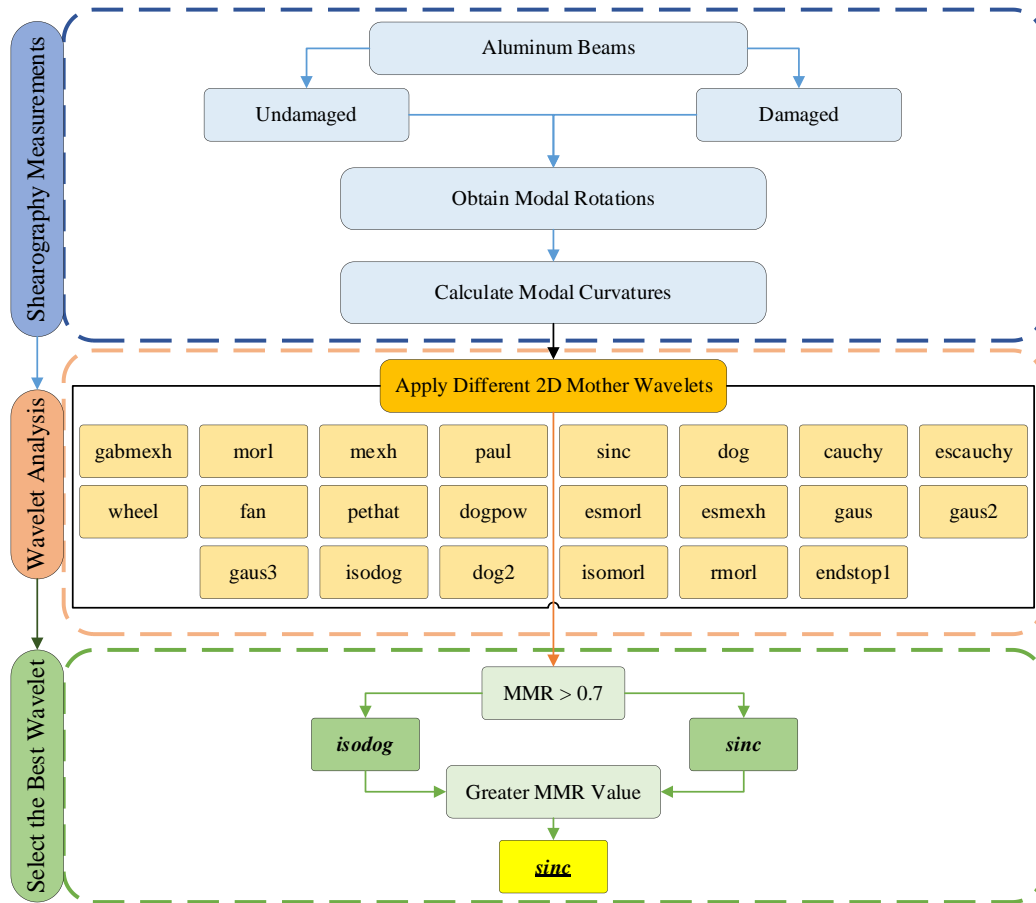


Fig. 9. The overall flowchart of the damage detection process.

## 4. Results

### 4.1. Damage Detection in B1

B1 aluminum beam has a single artificial damage in the middle of the beam length ( $X = 200$  mm) with the ratio of the depth of the slot to the thickness of the beam equal to 7%. To check the ability of different 2D wavelets to identify this damage, the difference between the modal curvatures of the first to third modes in beam B1 with their equivalent curvatures in the undamaged state, as an input to each of the wavelets. The coefficients obtained from the wavelets were evaluated as damage index ( $DI$ ) in three different scales of 1, 7, and 15. In this paper, the symbol  $WN\_MC\_Sn$  has been used to name the proposed damage indices. In this

symbol,  $WN$  represents the name of the applied wavelet,  $MC$  represents the input modal curvature ( $M1$ : first modal curvature,  $M2$ : second modal curvature,  $M3$ : third modal curvature, and  $SUM$ : the sum of the wavelet coefficients applied on three modal curvatures), and  $Sn$  shows the scale considered in the wavelet transformation ( $S1$ : scale 1,  $S7$ : scale 7 and  $S15$ : scale 15). Investigating the results showed that scale 7 has shown more appropriate responses among the three different scales than scales 1 and 15. Moreover, the results showed that among the 22 different wavelets, the most proper responses were taken from *sinc* and *isodog* wavelets. Figs. 10 and 11, respectively, show the results obtained by applying the *sinc* and *isodog* wavelets with a scale of 7 on the input data of beam B1.

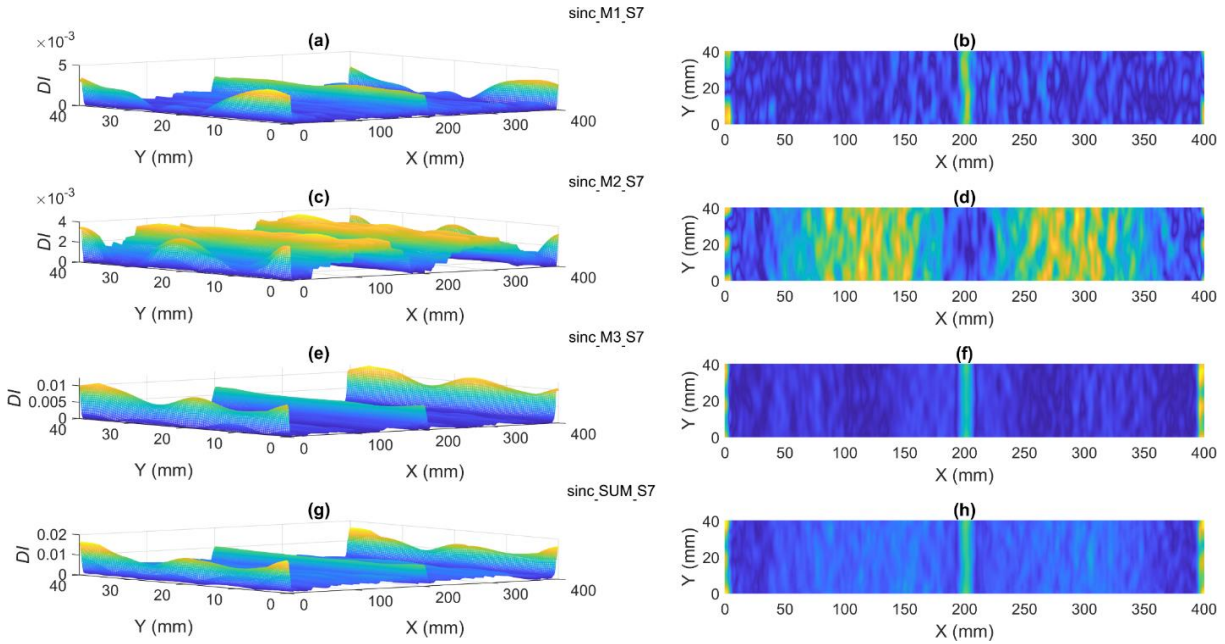


**Fig. 10.** 3D and 2D view of damage index ( $DI$ ) with sinc wavelet and scale 7 in B1: a & b) first model; c & d) second mode; e & f) third mode and g & h) summation of first three modes.

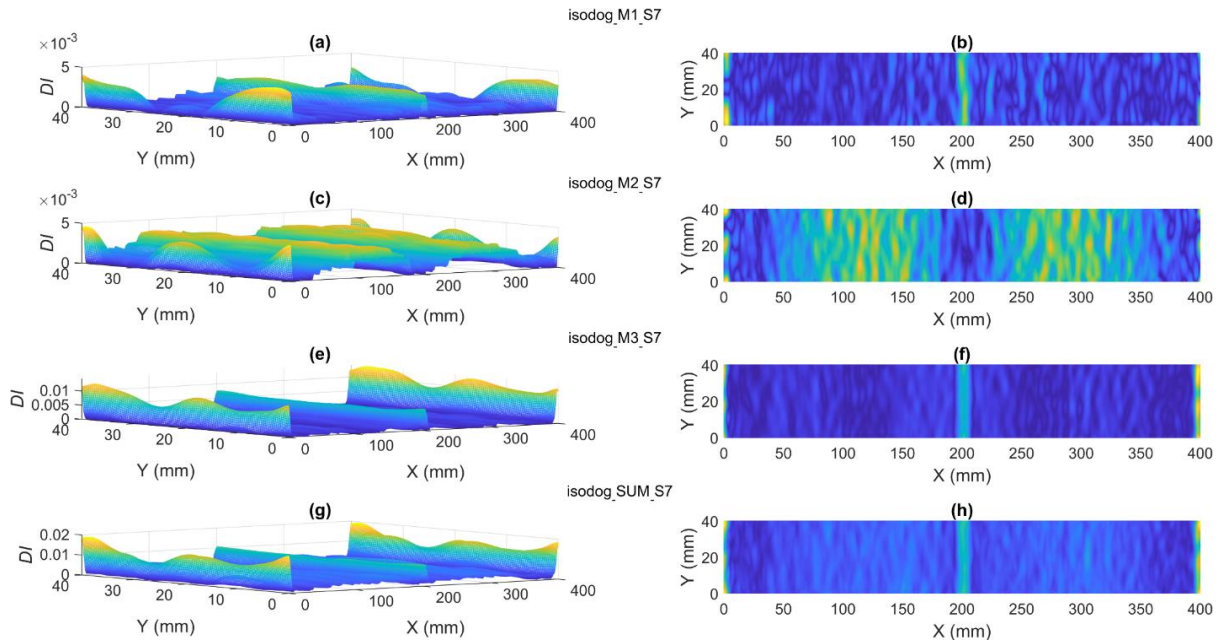


**Fig. 11.** 3D and 2D view of damage index ( $DI$ ) with isodog wavelet and scale 7 in B1: a & b) first model; c & d) second mode; e & f) third mode and g & h) summation of first three modes.

As seen in Figs. 10 and 11, the sinc and isodog wavelets were able to reveal the location of the damage in beam B1.

To show the obtained results of all utilized 2D wavelets, the average damage index profiles were introduced in this paper. These

profiles show the side view of the 3D damage indices that provide the average values of the damage index for different Ys for each X. In order to automatically determine the most suitable wavelets based on these profiles, the following two conditions have been applied:

The first and second peaks of the profiles show the place of damage scenarios.

The ratio of the maximum value of the wavelet coefficients in the middle part of the beams ( $Max_{Middle}$ : the section between the left and right sides of the beams on the horizontal axis) to the maximum value of the wavelet coefficients on the sides ( $Max_{Boundary}$ : a section measuring 25 mm from the right and left side of the horizontal X axis), named MMR is defined as the following relationship:

$$MMR = \frac{Max_{Middle}}{Max_{Boundary}} \quad (2)$$

The best wavelets were selected with an MMR ratio greater than 0.7

In Figs. 12 to 15, the name of the wavelets (1 to 22 different wavelets were utilized in this paper) along with the scale used (according to the predefined naming pattern WN\_MC\_Sn), the maximum value of the damage index on the sides (PB\_Val.), the value of the damage index in the first peak (PM1\_Val.) and the second peak (PM2\_Val.), along with the location of the first peaks (PM1\_Loc.) and the second peak (PM2\_Loc.) are presented for B1. In these figures, the profiles that had the two stated conditions were shown with green color and other profiles with red color.

As it can be concluded from Figs. 12 to 15, among the 22 different wavelets, the sinc and isodog wavelets were the ones with the best results in determining the locations of damages in B1.

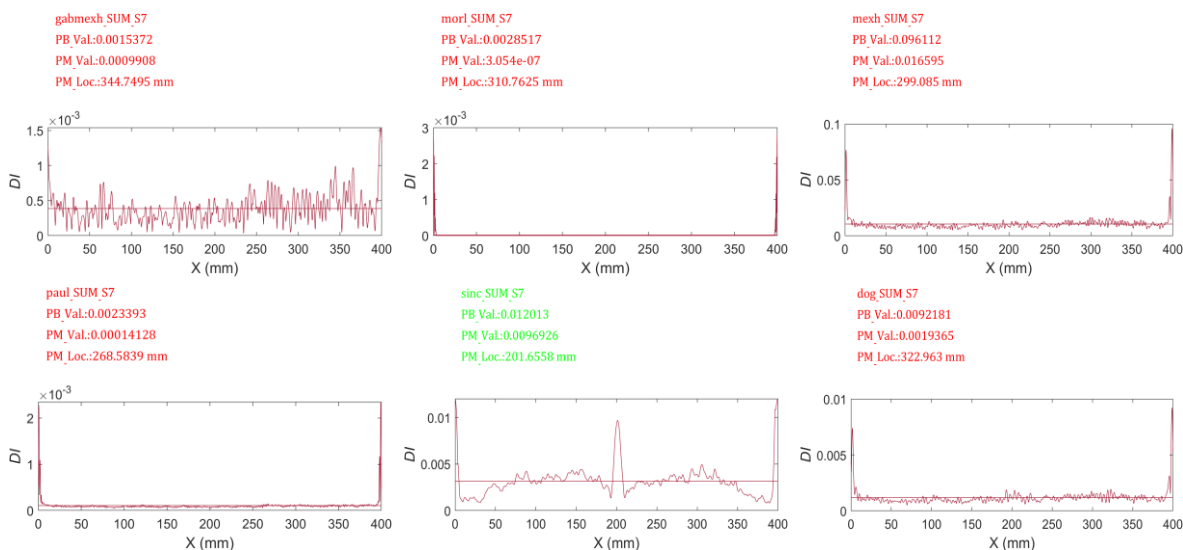


Fig. 12. Average profiles of damage index with scale 7 in beam B1 (wavelet number: 1-6).

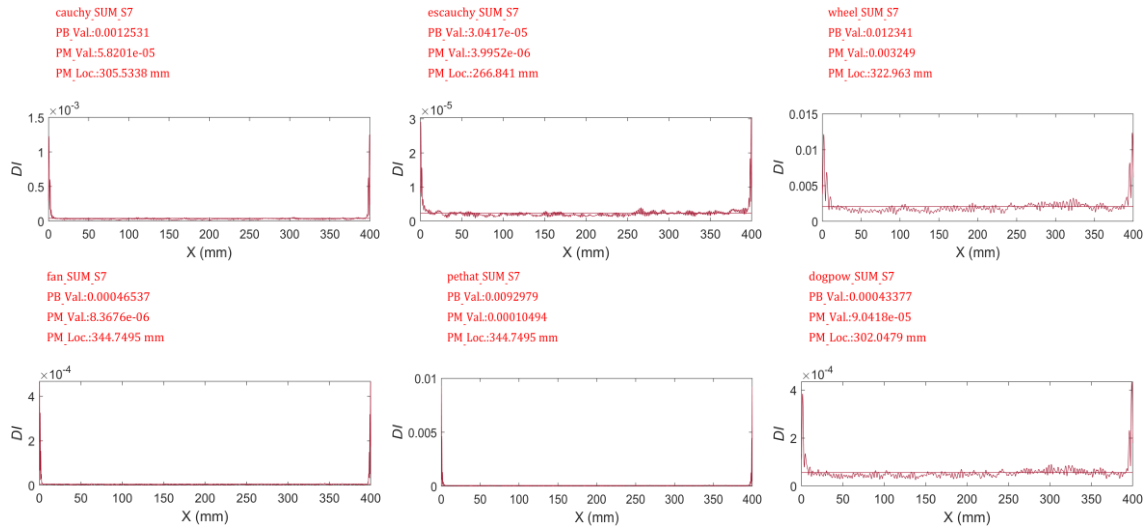


Fig. 13. Average profiles of damage index with scale 7 in beam B1 (wavelet number: 7-12).

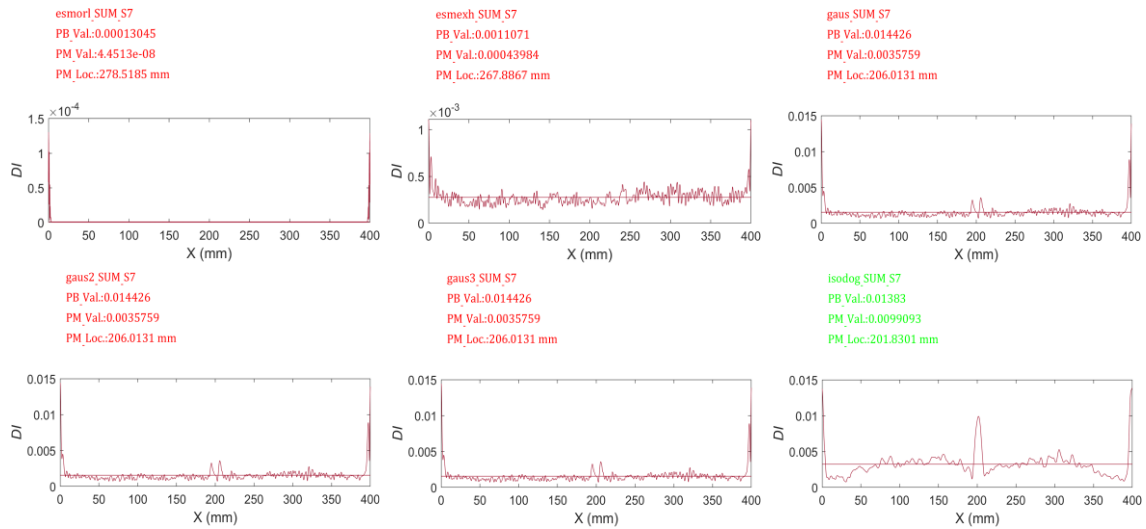


Fig. 14. Average profiles of damage index with scale 7 in beam B1 (wavelet number: 13-18).

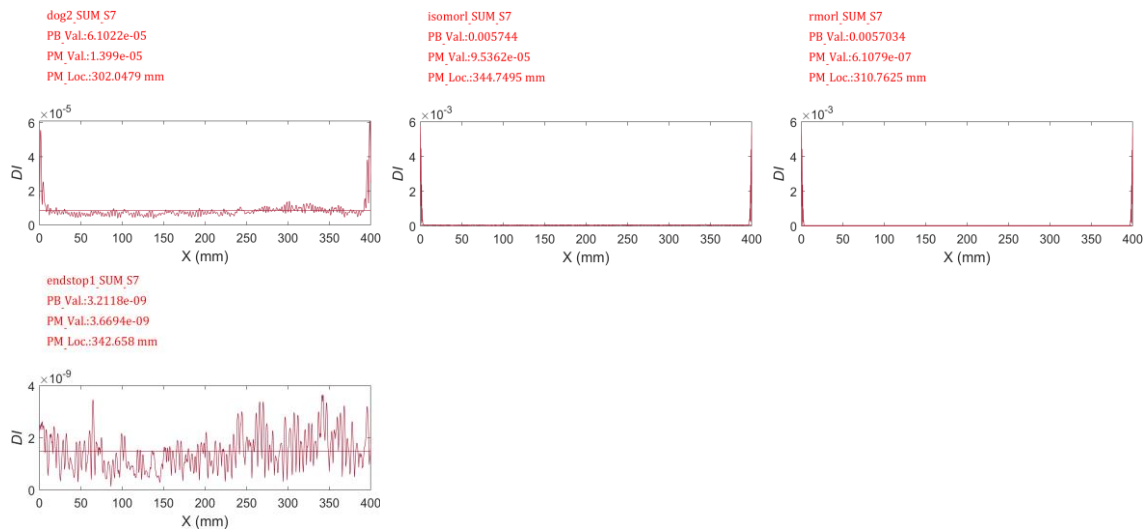


Fig. 15. Average profiles of damage index with scale 7 in beam B1 (wavelet number: 19-22).

## 4.2. Damage detection in B2

B2 aluminum beam has double slots in the middle of the beam length ( $X = 200$  mm) and its left side ( $X = 5.64$  mm) with the ratio of the depth of the slot to the beam thickness equal to 7%. Similar to beam B1, in order to investigate the ability of different 2D wavelets to identify the double damages of beam B2, the difference of the modal curvatures of the first to third modes in beam B2 with their equivalent curvatures in the undamaged state introduced as the input and the obtained wavelet coefficients were

evaluated as damage index ( $DI$ ) in three different scales 1, 7 and 15. Consistently to the results of B1, in B2 aluminum beam, the sinc and isodog wavelets with scale 7 revealed the most proper responses, which are illustrated in Figs. 16 and 17.

The overperforming of sinc and isodog wavelets among the other 22 utilized wavelets can be approved by investigating the 2D profiles illustrated in Figs. 18 to 21.

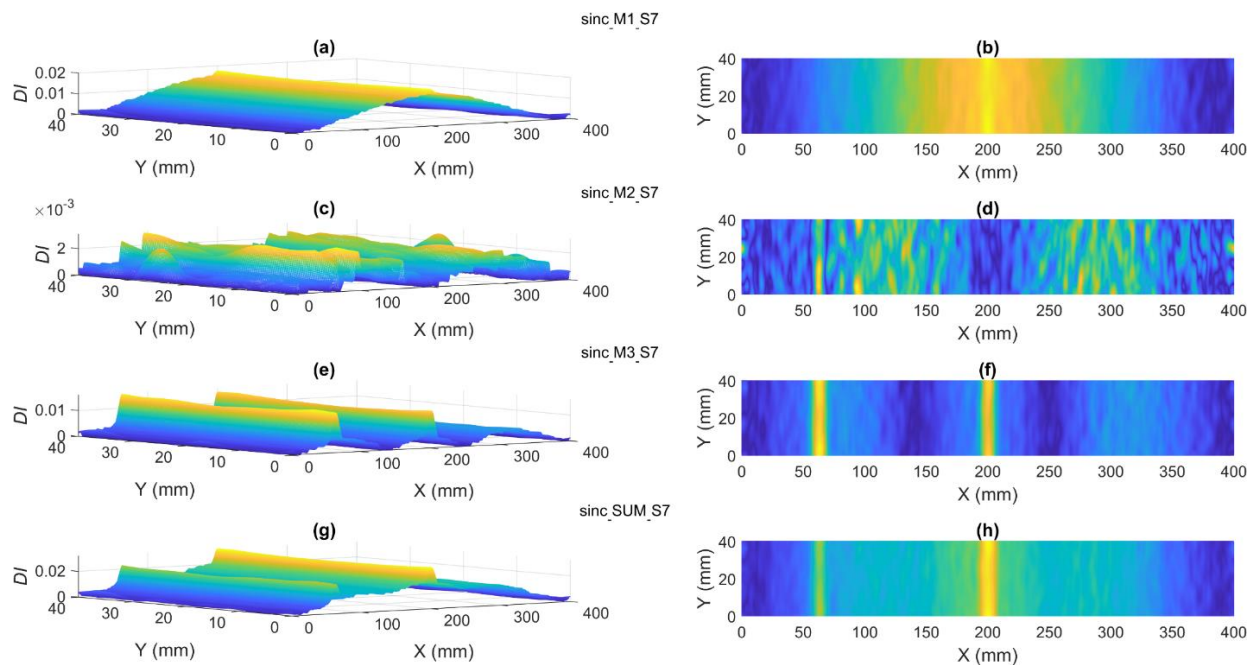


**Fig. 16.** 3D and 2D view of damage index ( $DI$ ) with sinc wavelet and scale 7 in B2: a & b) first model; c & d) second mode; e & f) third mode and g & h) summation of first three modes.



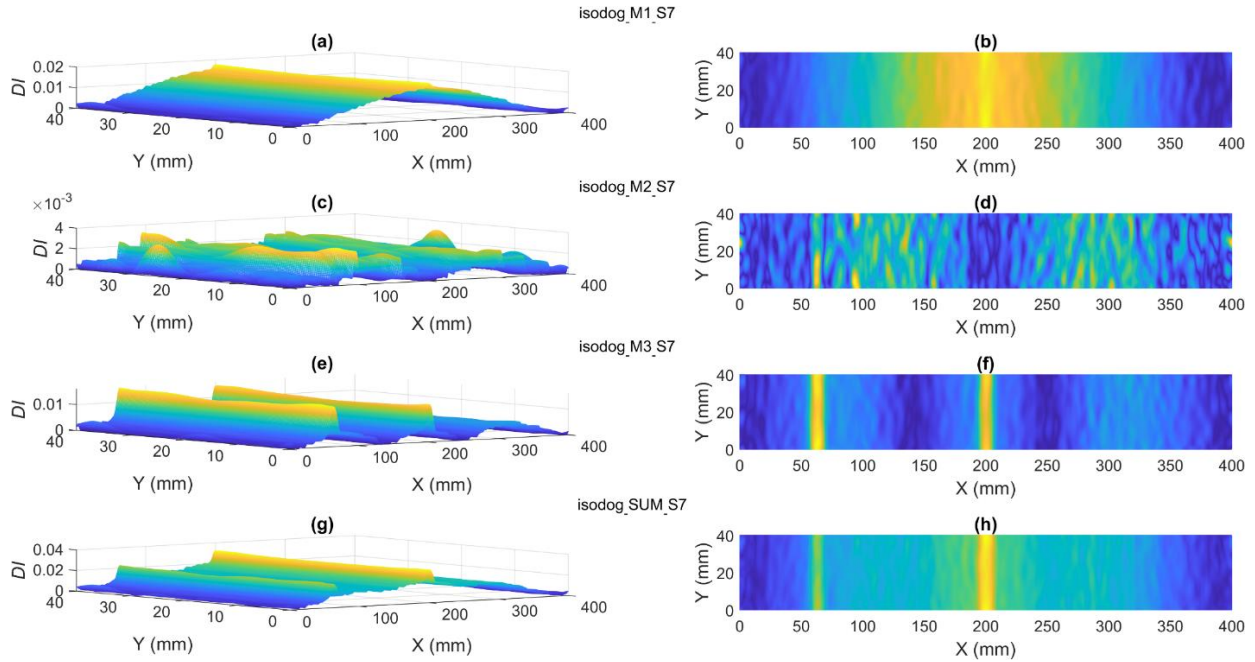


**Fig. 17.** 3D and 2D view of damage index ( $DI$ ) with isodog wavelet and scale 7 in B2: a & b) first model; c & d) second mode; e & f) third mode and g & h) summation of first three modes.

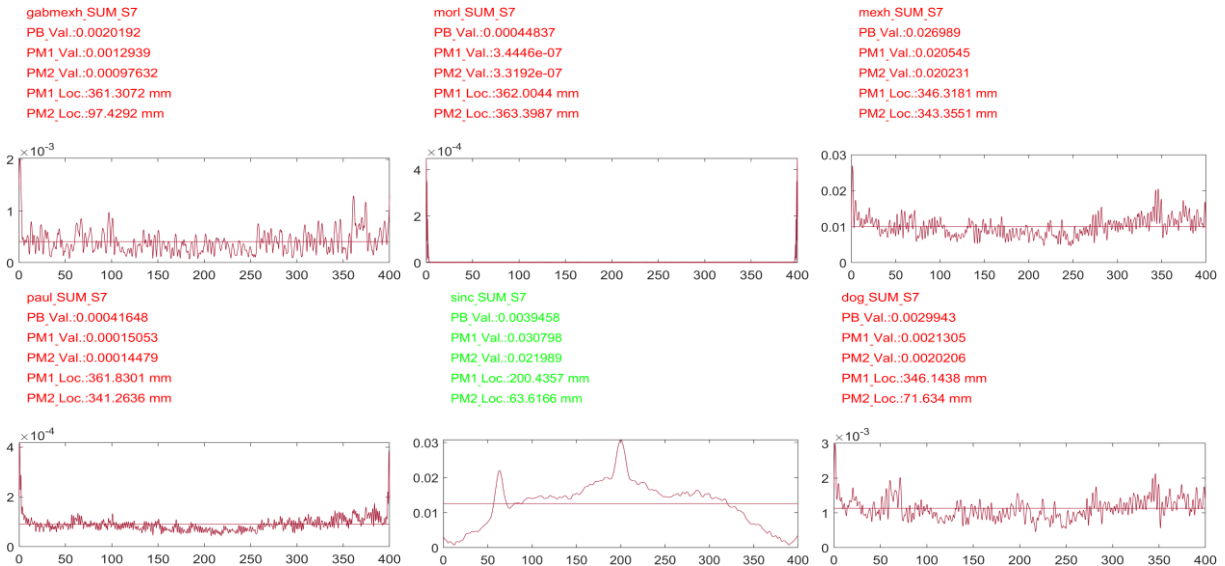


**Fig. 18.** Average profiles of damage index with scale 7 in beam B2 (wavelet number: 1-6).

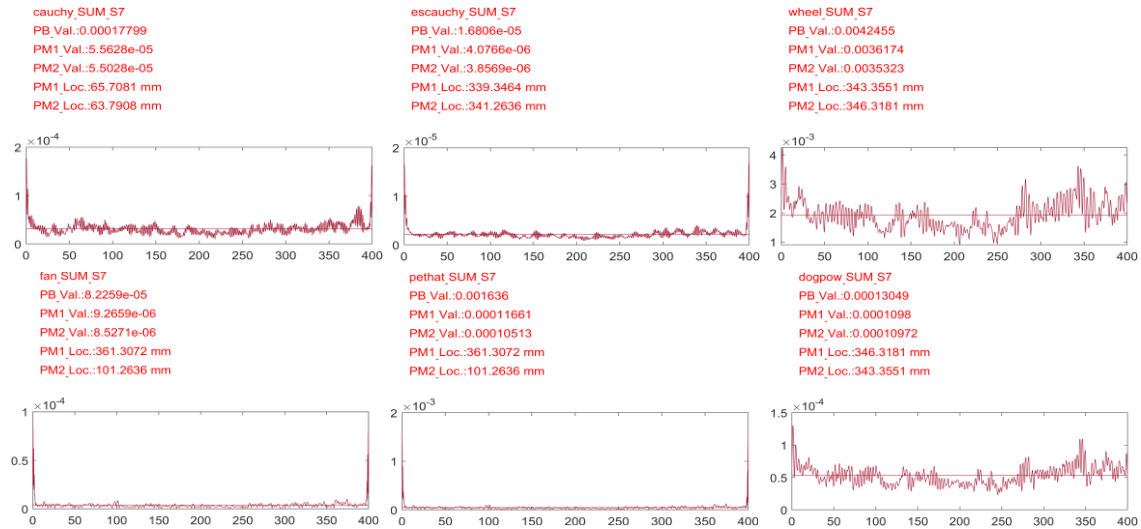


Fig. 19. Average profiles of damage index with scale 7 in beam B2 (wavelet number: 7-12).

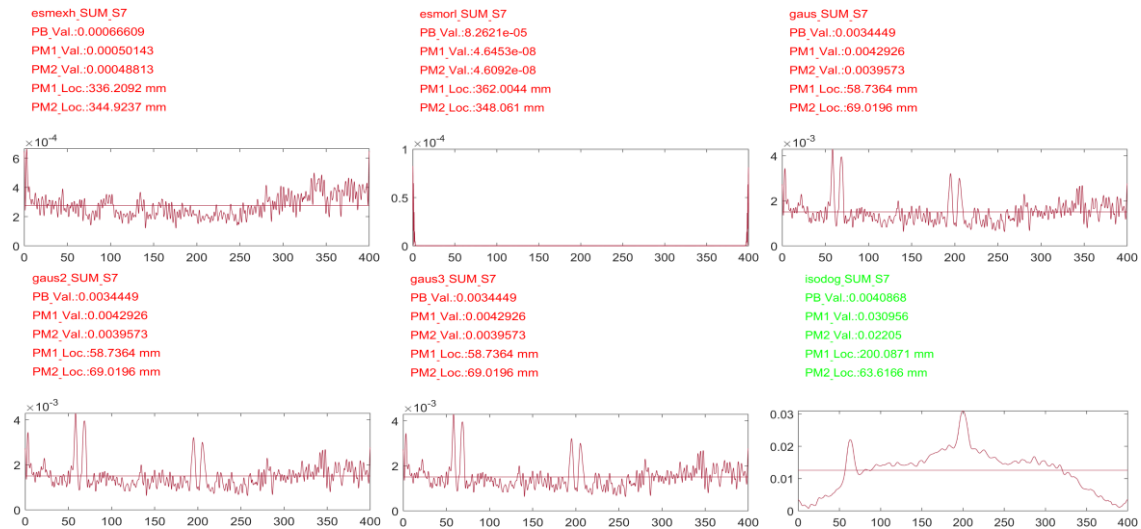


Fig. 20. Average profiles of damage index with scale 7 in beam B2 (wavelet number: 13-18).

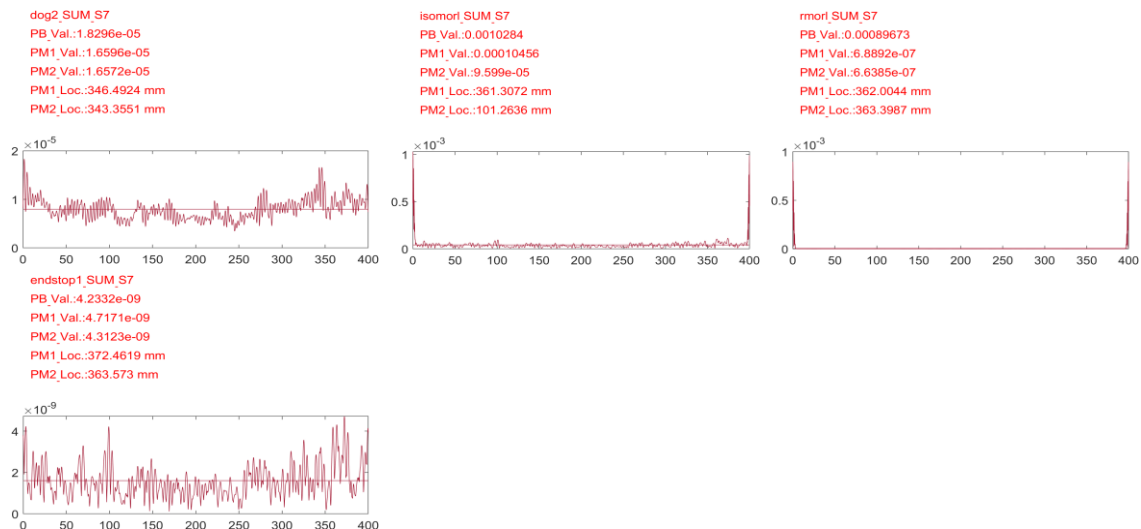
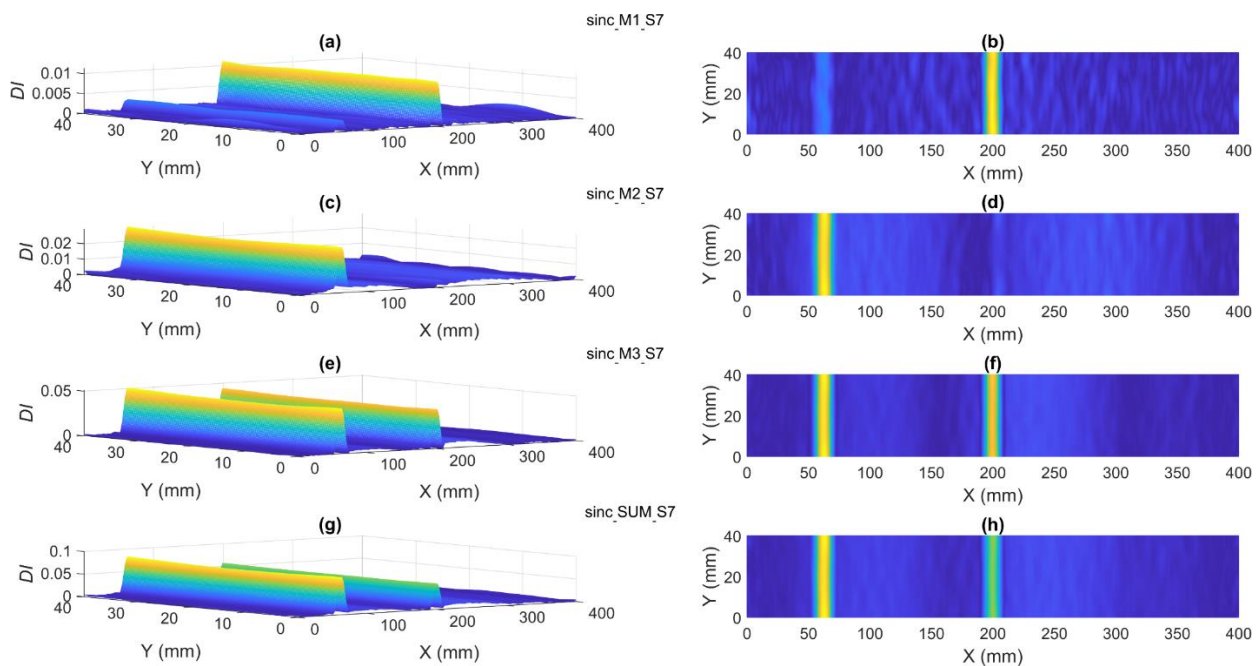


Fig. 21. Average profiles of damage index with scale 7 in beam B2 (wavelet number: 19-22).

### 4.3. Damage detection in B3

B3 aluminum beam, similar to the B2 beam, has two slots as damage scenario in the middle of the beam length ( $X = 200$  mm) and its left side ( $X = 64.5$  mm), but the ratio of the depth of the slots to the beam thickness in this beam is 30%. be Similar to beams B1 and B2, in order to check the ability of different 2D wavelets to identify the double damages of beam B3, the difference of the

modal curvatures of the first to third modes in beam B3 with their equivalent curvatures in the undamaged state were introduced as input to wavelet transform with scales 1, 7 and 15 and the obtained wavelet coefficients were named as damage index ( $DI$ ). The outcomes showed the same as B1 and B2, in B3 aluminum beam sinc and isodog wavelets with scale 7 lead to the best results as shown in Figs. 22 and 23, respectively, and also illustrated in profiles in Figs. 24 to 27.



**Fig. 22.** 3D and 2D view of damage index ( $DI$ ) with sinc wavelet and scale 7 in B3: a & b) first model; c & d) second mode; e & f) third mode and g & h) summation of first three modes.

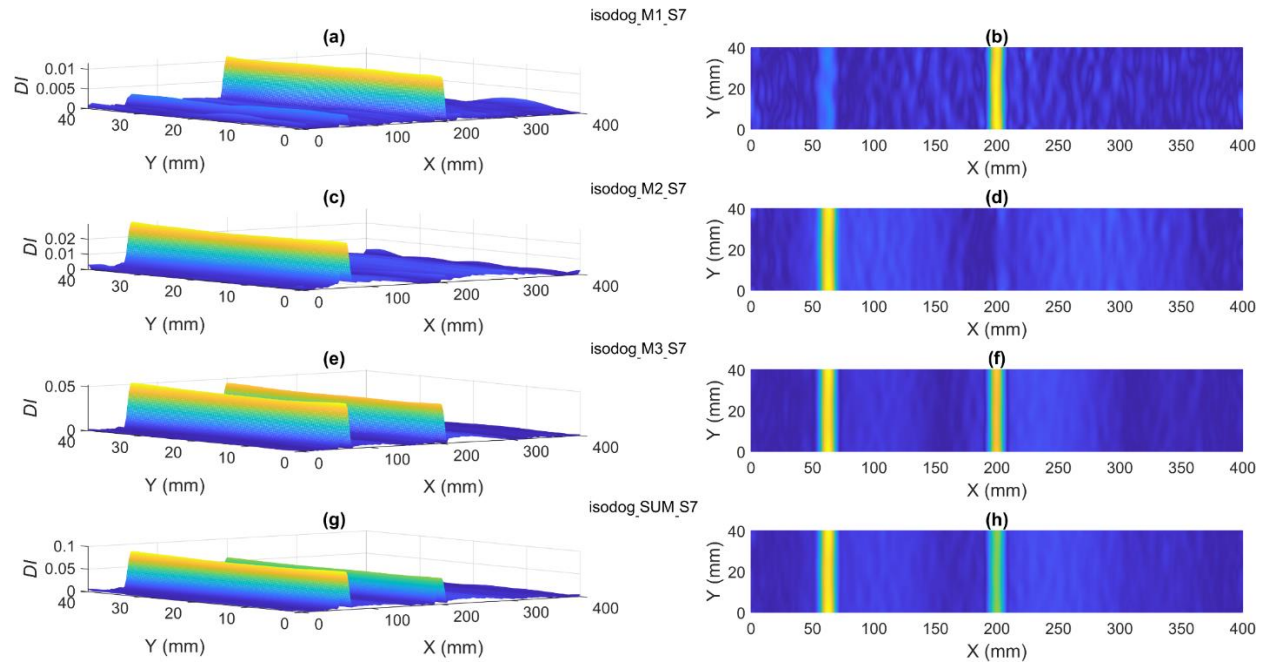


**Fig. 23.** 3D and 2D view of damage index ( $DI$ ) with isodog wavelet and scale 7 in B3: a & b) first model; c & d) second mode; e & f) third mode and g & h) summation of first three modes.

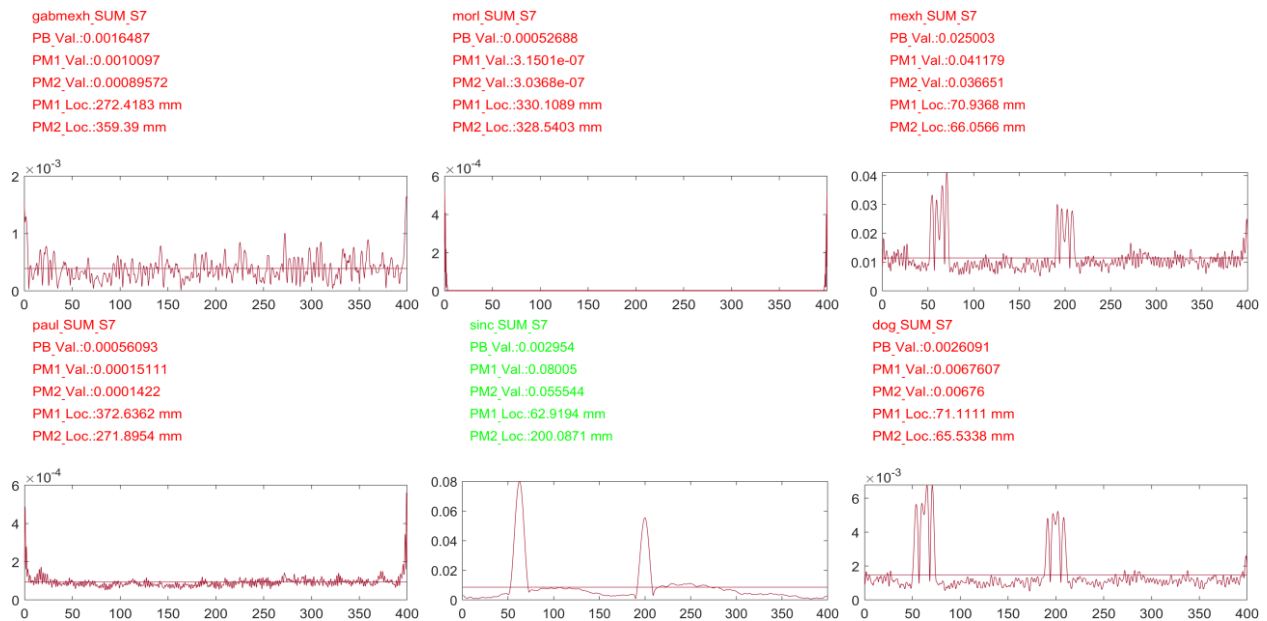


**Fig. 24.** Average profiles of damage index with scale 7 in beam B3 (wavelet number: 1-6).

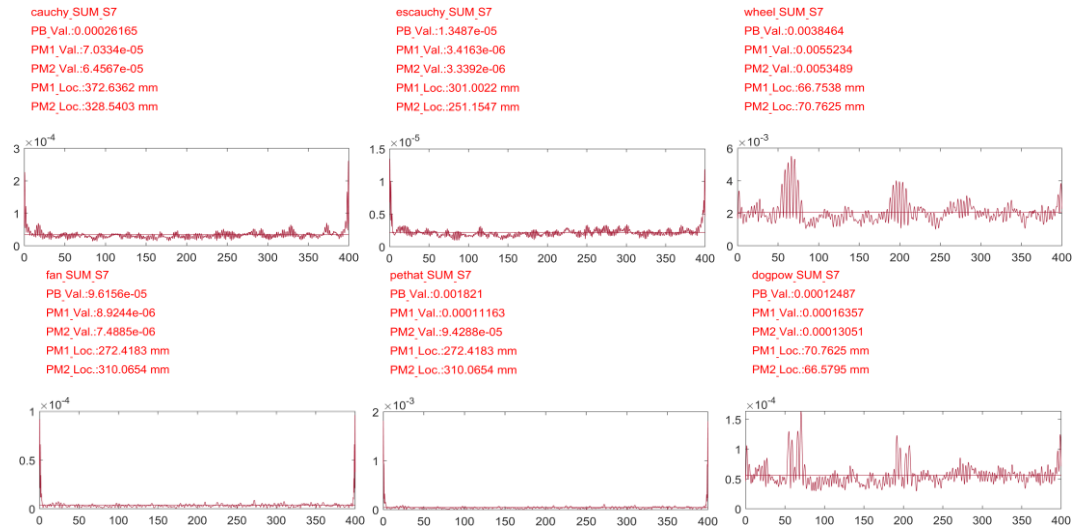


Fig. 25. Average profiles of damage index with scale 7 in beam B3 (wavelet number: 7-12).

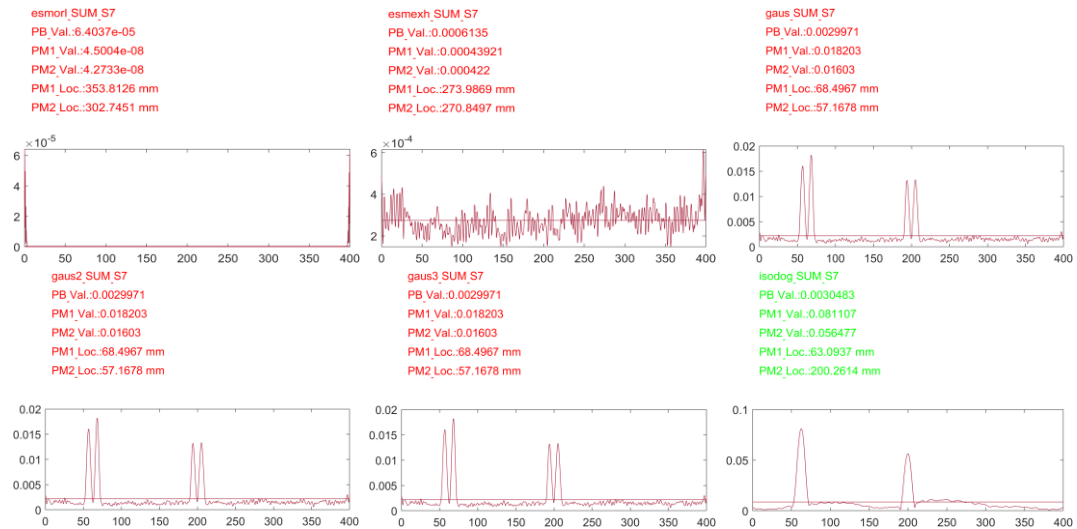


Fig. 26. Average profiles of damage index with scale 7 in beam B3 (wavelet number: 13-18).

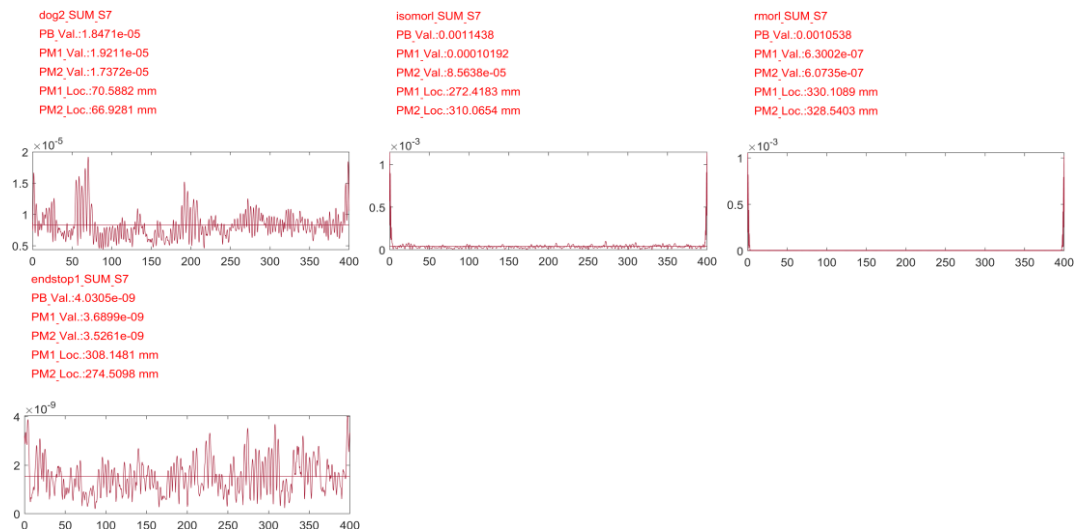


Fig. 27. Average profiles of damage index with scale 7 in beam B3 (wavelet number: 19-22).



#### 4.4. Best wavelet selection

As it is shown in sections 4.1 to 4.23, among different utilized 2D wavelets, only the sinc and the isodog wavelets have been able to reveal the location of the double damages and the rest of the wavelets did not have the ability to detect single and double damage in beams B1, B2, and B3.

To select the best wavelet between the sinc and isodog wavelets, the MMR ratios for all three B1, B2, and B3 beams are depicted in Fig. 28.

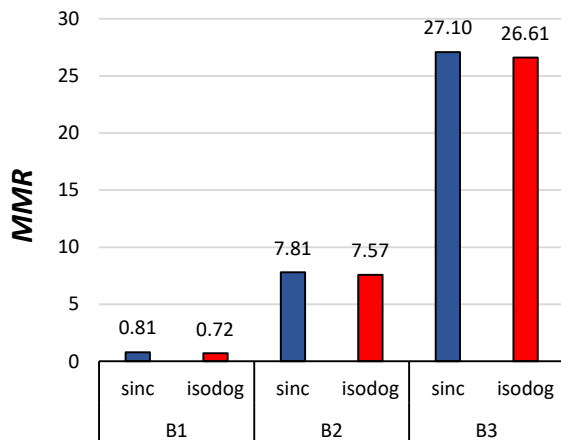


Fig. 28. MMR ratio calculated using sinc and isodog wavelets for different beams.

As shown in Fig. 28, in all three beams, B1, B2, and B3, the value of MMR ratios for sinc wavelet is higher than that of isodog wavelet. Therefore, it can be concluded that the sinc wavelet is more sensitive to damage scenarios than the isodog wavelet, and it can be considered the best wavelet for detecting damages in the tested aluminum beams.

## 5. Conclusion

In this research, aluminum beams with a length of 400 mm and a width of 40 mm in four undamaged states (B0), with single damage in the middle of the beam length (X

= 200 mm length) with the ratio of the depth of the crack to the thickness of the sheet equal to 7% (B1), with double damages in the middle of the beam (in length X = 200 mm) and the left side (in length X = 64.5 mm) of the beam with the ratio of the depth of the crack to the thickness of the sheet equal to 7% (B2) and with double damages in the middle of the beam (in length X = 200 mm) and the left side (in length X = 64.5 mm) of the beam were made with the ratio of the depth of the gap to the thickness of the sheet equal to 28% (B3). Then, with the help of shearography method, the modal data of each of them were taken in the form of modal rotations for the first to third mode shapes. By deriving the modal rotations, the modal curvatures were calculated for each of the mode shapes and introduced as the input of 22 different families of wavelet transforms with three different scales 1, 7, and 15, with their help, different states of damage in beams can be identified. The results of this research can be summarized as follows:

- The results showed that by deriving the mode shape, the sensitivity of the damage indicators increases. Based on this, considering the modal curvatures as the input of the wavelet transformation compared to the modal rotations and mode shapes themselves leads to the proper detection of most of the damages in the beams.
- The evaluation of the trial-and-error process showed that among scales 1, 7, and 15, considering scale 7 for wavelet families provides more appropriate outcomes.
- Comparison of the location of the first and second peaks of the average profiles

obtained from the coefficients of different families of 2D wavelets showed that sinc and isodog wavelet families can identify the location of damage scenarios in three cases of damages in B1, B2, and B3 aluminum beams.

- The results showed that between the best selected wavelets, sinc wavelet is more sensitive to damage scenarios than the isodog wavelet, and it can be considered the best wavelet for detecting damages in the tested aluminum beams.

## Funding

The authors have no funding to report.

## Conflicts of interest

The authors have no conflicts of interest to declare.

## Authors contribution statement

Amirhossein Abbasi: Conceptualization; Data curation; Formal analysis; Investigation; Methodology; Software; Validation; Visualization;

Mohsen Khatibinia: Conceptualization; Data curation; Formal analysis; Methodology; Resources; Supervision; Visualization; Writing – original draft; Writing – review & editing.

Hashem Jahangir: Conceptualization; Data curation; Formal analysis; Investigation; Methodology; Project administration; Resources; Software; Supervision; Validation; Visualization; Roles/Writing – original draft; Writing – review & editing.

José Viriato Araújo Dos Santos: Conceptualization; Data curation; Investigation; Methodology; Resources; Software; Validation; Visualization; Writing – original draft; Writing – review & editing.

Hernani Miguel Reis Lopes: Conceptualization; Data curation; Investigation; Methodology; Resources; Software; Validation; Visualization; Writing – original draft; Writing – review & editing.

## References

- [1] Cabboi A, Gentile C, Saisi A. From continuous vibration monitoring to FEM-based damage assessment: Application on a stone-masonry tower. *Construction and Building Materials* 2017;156:252–65. <https://doi.org/10.1016/J.CONBUILDMA.2017.08.160>.
- [2] García-Macías E, Kita A, Ubertini F. Synergistic application of operational modal analysis and ambient noise deconvolution interferometry for structural and damage identification in historic masonry structures: three case studies of Italian architectural heritage. *Structural Health Monitoring* 2020;19:1250–72. <https://doi.org/10.1177/1475921719881450>.
- [3] Fallah N, Hoseini Vaez SR, Esfandiari A. Damage identification of structures based on sensitivity equations using PCA and PSD data. *Proceedings of the Institution of Mechanical Engineers, Part C: Journal of Mechanical Engineering Science* 2022;095440622211388. <https://doi.org/10.1177/09544062221138846>.
- [4] Jahangir H, Khatibinia M, Mokhtari Masinaei M. Damage Detection in Prestressed Concrete Slabs Using Wavelet Analysis of Vibration Responses in the

- Time Domain. *Journal of Rehabilitation in Civil Engineering* 2022;10:37–63. <https://doi.org/10.22075/jrce.2021.23385.1510>.
- [5] Hanteh M, Rezaifar O. Damage detection in precast full panel building by continuous wavelet analysis analytical method. *Structures* 2021;29:701–13. <https://doi.org/10.1016/j.istruc.2020.12.002>.
- [6] Hanteh M, Rezaifar O, Gholhaki M. Selecting the appropriate wavelet function in the damage detection of precast full panel building based on experimental results and wavelet analysis. *Journal of Civil Structural Health Monitoring* 2021;11:1013–36. <https://doi.org/10.1007/s13349-021-00497-6>.
- [7] Entezami A, Sarmadi H, Behkamal B, Mariani S. Health Monitoring of Large-Scale Civil Structures: An Approach Based on Data Partitioning and Classical Multidimensional Scaling. *Sensors* 2021;21:1646. <https://doi.org/10.3390/s21051646>.
- [8] Livitsanos G, Shetty N, Verstryngge E, Wevers M, Hemelrijck D Van, Aggelis DG. Acoustic Emission Health Monitoring of Historical Masonry to Evaluate Structural Integrity under Incremental Cyclic Loading. *Proceedings* 2018;2. <https://doi.org/10.3390/ICEM18-05417>.
- [9] Ubertini F, D'Alessandro A, Downey A, García-Macías E, Laflamme S, Castro-Triguero R. Recent Advances on SHM of Reinforced Concrete and Masonry Structures Enabled by Self-Sensing Structural Materials. *Proceedings* 2018;2. <https://doi.org/10.3390/ecsa-4-04889>.
- [10] Katunin A, Araújo Dos Santos J V., Lopes H. Application of wavelet analysis to differences in modal rotations for damage identification. *IOP Conference Series: Materials Science and Engineering* 2019;561. <https://doi.org/10.1088/1757-899X/561/1/012024>.
- [11] Lopes H, Ribeiro J, Dos Santos AJV. Interferometric techniques in structural damage identification. *Shock and Vibration* 2012;19:835–44. <https://doi.org/10.3233/SAV-2012-0692>.
- [12] Francis D, Tatam RP, Groves RM. Shearography technology and applications: a review. *Measurement Science & Technology* 2010;21:102001. <https://doi.org/10.1088/0957-0233/21/10/102001>.
- [13] Zhao Q, Dan X, Sun F, Wang Y, Wu S, Yang L. Digital shearography for NDT: Phase measurement technique and recent developments. *Applied Sciences (Switzerland)* 2018;8. <https://doi.org/10.3390/app8122662>.
- [14] Akbari D, Soltani N, Farahani M. Numerical and experimental investigation of defect detection in polymer materials by means of digital shearography with thermal loading. *Proceedings of the Institution of Mechanical Engineers, Part B: Journal of Engineering Manufacture* 2013;227:430–42. <https://doi.org/10.1177/0954405412473054>.
- [15] Katunin A, Przystalka P. Damage assessment in composite plates using fractional wavelet transform of modal shapes with optimized selection of spatial wavelets. *Engineering Applications of Artificial Intelligence* 2014;30:73–85. <https://doi.org/10.1016/j.engappai.2014.01.003>.
- [16] Zhou J, Li Z, Chen J. Damage identification method based on continuous wavelet transform and mode shapes for composite laminates with cutouts.

- Composite Structures 2018;191:12–23.  
<https://doi.org/10.1016/j.compstruct.2018.02.028>.
- [17] Pnevmatikos N, Konstandakopoulou F, Blachowski B, Papavasileiou G, Broukos P. Multifractal analysis and wavelet leaders for structural damage detection of structures subjected to earthquake excitation. *Soil Dynamics and Earthquake Engineering* 2020;139:106328. <https://doi.org/10.1016/j.soildyn.2020.106328>.
- [18] Jahangir H, Hasani H, Esfahani MR. Wavelet-based damage localization and severity estimation of experimental RC beams subjected to gradual static bending tests. *Structures* 2021;34:3055–69. <https://doi.org/10.1016/j.istruc.2021.09.059>.
- [19] Khanahmadi M, Gholhaki M, Rezaifar O, Dejkam B. Damage identification in steel beam structures based on the comparison of analytical results of wavelet analysis. 2023 n.d.;8. <https://doi.org/10.22091/CER.2022.8340.1407>.
- [20] Fakharian P, Naderpour H. Damage Severity Quantification Using Wavelet Packet Transform and Peak Picking Method. *Practice Periodical on Structural Design and Construction* 2022;27. [https://doi.org/10.1061/\(ASCE\)SC.1943-5576.0000639](https://doi.org/10.1061/(ASCE)SC.1943-5576.0000639).
- [21] Katunin A, Araújo dos Santos JV, Lopes H. Damage identification by wavelet analysis of modal rotation differences. *Structures* 2021;30:1–10. <https://doi.org/10.1016/j.istruc.2021.01.010>.
- [22] Katunin A, Lopes H, dos Santos JVA. Identification of multiple damage using modal rotation obtained with shearography and undecimated wavelet transform. *Mechanical Systems and Signal Processing* 2019;116:725–40. <https://doi.org/10.1016/j.ymsp.2018.07.024>.
- [23] Araujo dos Santos J V., Katunin A, Lopes H. Vibration-Based Damage Identification Using Wavelet Transform and a Numerical Model of Shearography. *International Journal of Structural Stability and Dynamics* 2019;19:1950038. <https://doi.org/10.1142/S021945541950038X>.
- [24] Smith M. ABAQUS/Standard User's Manual, Version 6.9. Simulia; 2009.
- [25] Cinque D. Machine learning techniques for damage identification in beams. Università degli Studi Roma Tre, 2019.